Available online at www.sciencedirect.com
SCIENCE DIRECT®
Polymer 44 (2003) 4817–4827
polymer
www.elsevier.com/locate/polymer

# Side-chain motions in poly(methyl methacrylate) + $SiO_2$ hosts of fluorescent dyes studied by thermally stimulated discharge currents: effects of confinement and blending

Ioannis M. Kalogeras

*Section of Solid State Physics, Department of Physics, University of Athens, Panepistimiopolis, 157 84 Zografos, Hellas, Greece*

Received 14 January 2003; received in revised form 28 May 2003; accepted 5 June 2003

**Abstract**

The thermally stimulated discharge (TSD) currents technique has been used to study different types of inter- and intra-molecular interactions between the components in poly(methyl methacrylate) (PMMA)-based systems. The TSD current signal of the side-chain dielectric β relaxation mode of PMMA has been comparatively studied in bulk PMMA, PMMA polymerized in-situ mesoporous silica-gel, and these matrices in the presence of polar and ionic (rhodamine 6G/$Cl^-$) or non-polar (perylene derivatives) fluorescent dyes. The analysis of the TSD responses by means of partial heating and thermal sampling techniques indicates that polymer's confinement in $SiO_2$ induces, firstly, an increase of the distributed energy barriers of the β relaxation mode, and secondly, an enhancement of the contribution of the faster relaxation modes (at $T < T_{max(\beta)}$) in the overall strength of the β mechanism. Basic features of the β bands (i.e. peak maximum and distribution of activation energies) exclude the occurrence of strong interactions between the perylene derivatives and the carbonyl groups of PMMA. To contrary, coupling effects appear between the motions of the side-groups of PMMA and rhodamine 6G. The results are interpreted in view of counteracting structural (e.g. modification of the polymer's free volume) and surface (hydrogen-bond interphase interactions) effects of confinement and blending on the relaxation dynamics of the pendant groups.


*Keywords:* Polymethyl methacrylate; Dyes; Nanocomposites

## 1. Introduction

Laser dyes can be incorporated into various liquid or solid-state matrices [1]. Despite the fact that tunable lasers based on static or flowing liquid systems are inconvenient in use there is ongoing interest for such systems for a number of reasons. Typical advantages of the liquid dye carriers are their ability, with the availability of dyes, to cover the spectrum from the ultra-violet (UV) to the infrared (IR) with exceptional performance, their operation from continuous-wave to mode-locked picosecond regimes and from low to high average powers, the minimization of heat dissipation problems as well as the relatively low cost of the laser apparatus. However, given that the host adversely affects many thermodynamic, spectroscopic and kinetic properties of the dye, intense interest has recently emerged for the use of suitable solid-state laser devices in conjunction with the implementation of efficient and photostable dyes.

Attempts to develop optical components based on solid-state matrices with embedded dyes were initially concentrated on transparent polymers, but without promising results. Furthermore, the encapsulation of thermally dissociative non-linear, ferroelectric or organic components in glass products of oxide-particles melting procedures has never been realized due to the use of high melting temperatures (ca. 1150 °C for $SiO_2$). In recent years the sol–gel process has offered an important low-temperature processing route for the preparation of glasses with desired low-density structures, maintaining at the same time a high degree of purity and homogeneity [2]. The sol–gel processing chemistry is mainly based on inorganic polymerization reactions at temperatures near ambient, which are initiated by organometallic molecular precursors, such as liquid silicon alkoxides $Si(OR)_n$ where R is an alkyl group. Silica-gel's structural evolution proceeds via nucleophilic

*E-mail address:* ikaloger@cc.uoa.gr (I.M. Kalogeras).

0032-3861/03/$ - see front matter © 2003 Elsevier Science Ltd. All rights reserved.
doi:10.1016/S0032-3861(03)00498-1

substitution reactions, such as hydroxylation (hydrolysis) of tetraalkoxysilane

$$Si(OR)_4 + 4H_2O \rightarrow Si(OH)_4 + 4ROH$$

and mineral acid (e.g. $HNO_3$) or basic (e.g. $NH_3$) catalyzed (poly)condensation reactions

$$nSi(OH)_4 \rightarrow (SiO_2)_n + 4nH_2O$$

to form ≡Si–O–Si≡ bonds, until the construction of a sol with a local $SiO_2$ network. The sol particles link in gelation to form a three-dimensional wet gel structure. Carefully controlled drying processes result to partially of fully densified silicas [2].

Over the past years, several laser dyes have been incorporated into silica gels, xerogels, alumina gels and other sol–gel process derived glasses. Such solid-state dye laser materials were intensively tested by measuring optical characteristics, like, optical scattering, fluorescence quantum yield, efficiency, tunability in pump wavelength and photostability. The porous nature of partially densified sol–gel inorganic glasses permits them to perform as excellent thermally, chemically and dimensionally stable carriers of organic substances with optical functions, such as fluorescence, phosphorescence, photoconductivity, laser oscillation and non-linear optical properties. In contradiction to plastic carriers and organic solvents, the encapsulation of the laser dye molecules into a silica-gel matrix [3–8] has provided an inert and non-hazardous medium for solid-state dye lasers, by making compact, versatile, non-volatile, non-flammable, non-toxic and inexpensive systems with the capability to entrap the dye molecules within the matrix with maintained physical and chemical properties [4,9]. For a range of industrial applications, the functionality of the sol–gel process derived porous systems can be largely improved by incorporating a suitable environmentally stable and optically transparent organic phase, such as poly(methyl methacrylate) (PMMA) [10–15], into the silica-gel skeleton for the fabrication of dense inorganic–organic composites. These dual-matrix materials possess a range of advanced physico-chemical properties [10–12] and multifunctional photonic or mechanical applications, e.g. higher optical quality and energy laser action; higher strength, fracture toughness and abrasion resistance; increased thermal conductivity, thermal expansion and thermal shock resistance; easiest shaping and optical polishing by conventional methods. The organic phase also serves as a coating to prevent undesired substances such as atmospheric water from contaminating the highly hydrophilic porous matrix [11]. This is possible due to the 'elimination' of the accessible adsorbing sites provided by the silanols at the silica surface [16].

The analysis of the molecular relaxation mechanisms in polymeric, inorganic and composite dye systems might give valuable information on the type and extent of the physical and chemical guest (dye)–host interactions. In particular, studies aiming to obtain better knowledge of the dielectric and electrical properties of PMMA in PMMA-based hosts of luminescent organics present both theoretical and practical significance, especially if one considers that the development of more efficient and photochemically stable solid-state dye laser systems is constant pursuit in the field of commercial applications. So far, a number of reports have focused on the dielectric and electrical properties of PMMA hosts of some fluorescent laser dyes, such as K1 [17], rhodamine 6G [17] rhodamine B [17], fluorescein-Na [18,19], coumarin 6 [18,19] and 4-[ethyl(2-hydroxyethyl)-amino]-4′-nitroazobenzene [20]. In these studies, several changes in the dielectric parameters (e.g. the activation energy, the distribution of the relaxation times and the dielectric strength) of the primary (α) and the secondary (β) relaxation mechanisms of PMMA were interpreted with respect to the range of intermolecular interactions between the macromolecular phase and the organic laser dyes. In parallel, PMMA's confinement in silica-gels is expected to influence several intrinsic relaxation modes. The literature presents contradictory results related to the effects of the restricted geometry on the molecular relaxation dynamics of confined glass-forming liquids and the molecular diffusion properties, compared to those of the bulk-liquid state. The scientific knowledge is undoubtedly less developed for complex systems involving glassy polymers embedded in micro- or mesoporous matrices [12,13,21–27], where most of the studies concentrate on the behavior of α transitions. In general, the effects on the molecular dynamics of the confined phase can be categorized to: structural effects due to the variations of the steric hindrances in the limited volume, surface effects owing to the wide range of molecular interactions at the phase boundaries, finite-size effects due to the spatial heterogeneity of the confined material, and simple mixture effects related to the topology, degree of order and dimensionality of the confining phase [28]. Their relative significance depends on several factors, such as the chemical nature of the phases, the porosity and the local inclusion geometry of the matrix.

In this article we present a dielectric study performed by means of the thermally stimulated discharge (TSD) currents technique [29] in a range of PMMA-based materials: amorphous PMMA, biphasic PMMA + $SiO_2$ composites (PMMA polymerized in situ 5 nm silica gels), and these matrices with dispersed laser-active organic dyes (Fig. 1). Confinement and blending effects on the secondary (β) relaxation process of PMMA have been investigated and the relative importance of the various types of interactions between the components will be discussed in connection with optical characteristics of the lasing matrices.

## 2. Experimental

TSD currents is a sensitive dc technique frequently used for the rapid characterization of materials through their dielectrically-active relaxation phenomena [30,31]. The

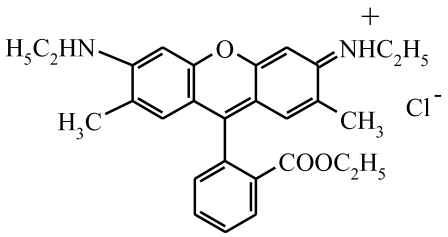


(a)

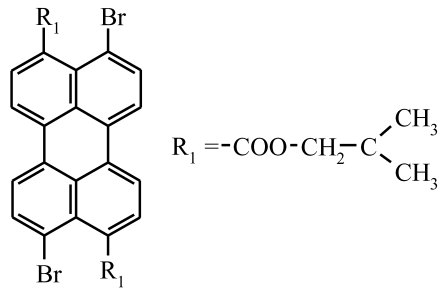


(b)

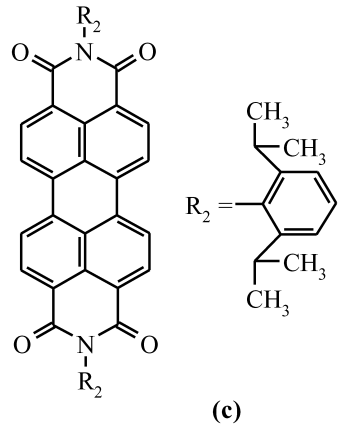


(c)

Fig. 1. Molecular structures of the polar and ionic (a) rhodamine 6G/$Cl^-$ (R6G), and the non-polar (b) perylene green (PG) and (c) perylene orange (PO) dyes.

technique is widely recognized as an efficient route for the determination of intra- and inter-molecular interactions in polymer-based composites, mostly by monitoring their effects on intrinsic dielectric relaxation mechanisms (e.g. dipolar, space charge and interfacial polarizations) of the starting materials.

In TSD the restoration of the non-polarized state of the dielectric material is monitored as a function of temperature with the aim to determine the origin of the relaxations involved and their kinetic parameters. Applying an electric field $E_p$ (polarizing field) for time $t_p$ (isothermal polarization time) at a suitable constant temperature $T_p$ (polarization temperature) generates the thermoelectret. The electric stimulus causes an alignment of permanent or induced dipoles as well as a drift of real charges (homo or heterocharges). The sample is then cooled down to a temperature $T_0(\ll T_p)$ at which the orientation of the dipoles may be frozen-in and charges may be trapped. These mechanisms decay in a short time either when heated up, with a constant rate $b$, or upon aging. By monitoring the TSD as a function of temperature, phase transitions as well as ionic and molecular motions in the polymer can be studied. For a single relaxation mechanism the recovery of the system produces an asymmetric discharge current density band, $J(T)$, which is described by

$$J(T) = A\exp\left\{-\frac{E_a}{RT} - \frac{B}{b}\int_{T_0}^{T}\exp\left[-\frac{E_a}{RT}\right]dT\right\} \quad (1)$$

where $R$ is the gas constant. The expressions for the adjustable parameters $A$ and $B$ vary depending on the exact process (determined by dipoles or space charges) involved in the release of the current. The actual expression of the thermostimulated discharge current also depends on the relationship used for the temperature dependent relaxation time. At temperatures below the glass–rubber transition temperature ($T_g$) of the amorphous phase of a polymer, the Arrhenius law is mostly used

$$\tau(T) = \tau_0\exp\left(\frac{E_a}{RT}\right) \quad (2)$$

where $E_a$ (in kJ/mol) is the activation energy, and $\tau_0(s)$ is the pre-exponential factor. Eq. (1) is deduced with use of Eq. (2). Independent of the actual $\tau(T)$ dependence there is a general relation between $B$ and the temperature corresponding to the maximum current, $T_{max}$

$$B = \frac{bE_a}{RT_{max}^2}\exp\left(\frac{E_a}{RT_{max}}\right) \quad (3)$$

For a molecular or an impurity-vacancy dipolar relaxation mechanism $B$ equals $\tau_0^{-1}$. In addition, parameters $A$ and $B$ are connected through the identity $A = P_0B$, where $P_0$ is the saturation polarization. For sub-glassy relaxation mechanisms in polymers deviations of the experimental TSD current peaks from the theoretical curve described by Eq. (1) are frequently attributed to a distribution of Arrhenius-type relaxation times $\tau(T)$ [30,31].

TSD current scans covered the range 10–320 K and were performed in vacuum between $10^{-1}$ and $10^{-4}$ Pa. The typical experimental conditions are: $T_p = 320$ K, $E_p = (3–5)\times 10^6$ V/m, $t_p = 5$ min and $b = 5°$/min (cooling/heating rate). Details on the experimental apparatus are given elsewhere [32].

The oligomeric organic components can be incorporated into the sol–gel matrix by two broadly different ways, either at the mixing stage of the sol–gel process or after the formation of the gel. The latter method creates polymer + inorganic oxide composites in which both the inorganic and organic parts physically coexist and can be chemically

identified. The incorporation of the dyes in PMMA and the composite PMMA + $SiO_2$ matrices was performed following different procedures. The non-polar perylene derivatives (Fig. 1b and c) were impregnated into the silicon oxide skeleton (nominal pore diameter 5 nm, total pore volume 0.7 $cm^3/g$, surface area of 580 $m^2/g$, bulk density 0.9 $g/cm^3$) simultaneously with the organic monomer (methyl methacrylate, MMA). Polymerization proceeded at 313 K for 3 days, initiated by 0.125% by mass of benzoyl peroxide dissolved into the MMA. Bulk PMMA and the PMMA + $SiO_2$ samples were prepared with similar polymerization conditions, in the absence of the dyes. The highly ionic and polar xanthine dye rhodamine 6G/$Cl^-$ (R6G, Fig. 1a) is only slightly soluble in the less polar MMA. Thus, for the impregnation of the $SiO_2$ substrate with R6G the following procedure has been used: the porous glass was immersed in ethanolic solution of R6G, for 2 weeks at a constant temperature of 313 K, followed by heat treatment in vacuum (at 413 K) in order to evaporate the solvent. Finally, the glass was immersed in the initiator-monomer solution and the mixture was sealed in a test tube under air and heated to 313 K. The R6G + PMMA blend was prepared by mixing ethanolic solution of the dye with the initiator–monomer mixture and polymerizing as above. The estimated dye concentrations (in mol/l, M) in the various blocks are listed in Table 1.

## 3. Results

PMMA is a typical polar thermoplastic with a collection of relatively well-established relaxation modes, denoted as α, β and γ, in order of decreasing peak temperature in the TSD spectra, and conversely, increasing relaxation frequency at isothermal dielectric relaxation spectroscopy (DRS) studies. The glass transition α process (at $T_g$, with TSD current maximum $T_\alpha$ around 378 K for atactic PMMA [13,15]) is ascribed to a long-range conformational change of the polymer backbone with cooperative motions involving between 8 and 20 bonds. The β relaxation mode corresponds to localized conformational changes that require motion about only one or two bonds. Bearing in mind the chemical structure of PMMA, the molecular mechanism of this sub-glassy relaxation signal is usually associated with the partial rotations of the ester group ($COOCH_3$) around the C–C bond linking the group to the main chain [33]. The secondary relaxation produces strong ac or dc dielectric and mechanical relaxation signals; their intensity depends, firstly, on the number of lateral groups for which rotation is possible, and secondly, on the steric hindrances exerted on the groups by adjacent methyl groups in the main chain and other surrounding molecular species. Fig. 2 shows the TSD current spectra of PMMA, and its blends with the luminescent dyes PG, PO and R6G (Fig. 1). The spectra contain a broad β relaxation band, in the temperature range 160–275 K with peak maximum at $T_\beta = 232 \pm 1$ K. For R6G + PMMA, in particular, the β relaxation is drastically downshifted to 223 ± 1 K. The band around 125 K is ascribed to a rotational relaxation mode from polar water molecules adsorbed in the polymeric phase [31] and the weak band at $T_\gamma = 70$ K is attributed to the γ relaxation of the α-methyl groups ($-CH_3$ groups covalently bonded to the macromolecular chains of PMMA).

In the biphasic PMMA + $SiO_2$ matrix the secondary relaxation band peaks at $T_\beta = 217 \pm 1$ K and in the dye + composite blends at 225 ± 2 K (Fig. 3). The low-temperature shift of the secondary relaxation band in PMMA + $SiO_2$, compared to the same signal in bulk PMMA, appears regardless of the type and the amount of the initiation used in the polymerization process [13]. Apart from the drastic downshift of the β band, the dielectric behavior of the PMMA and PMMA + $SiO_2$ hosts of the ionic rhodamine 6G/$Cl^-$ dye shows two unique characteristics: intense relaxation signals above approximately 270 K and a strong $H_2O$ relaxation band. Both mechanisms retain considerable dielectric strength even after prolonged water desorption (2 months in high vacuum at 320 K). The high-temperature signal in particular is related to the ionic

Table 1
Estimated dye concentrations in the purely organic (PMMA) and the composite (PMMA + $SiO_2$) matrices

| | Dye concentrations (M) | | |
|---|---|---|---|
| | Perylene green | Perylene orange | Rhodamine 6G/$Cl^-$ |
| PMMA | $5 \times 10^{-5}$ | $8 \times 10^{-5}$ | $8 \times 10^{-5}$ |
| PMMA + $SiO_2$ | $3 \times 10^{-5}$ | $7 \times 10^{-15}$ | $12 \times 10^{-5}$ |

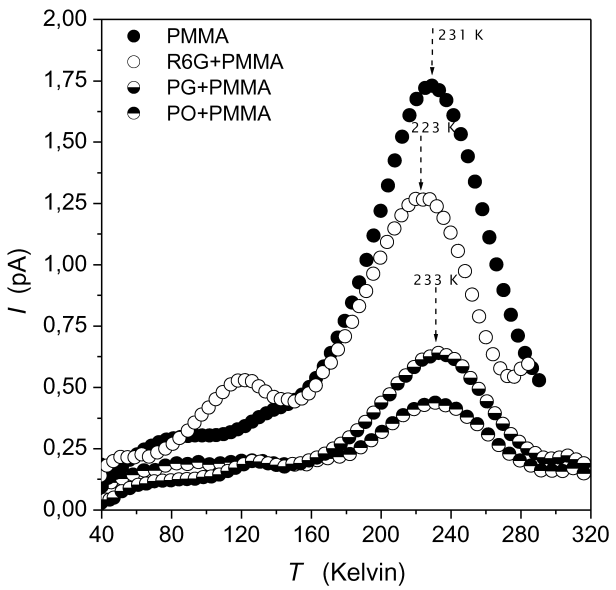


Fig. 2. TSD current spectra of bulk PMMA, PG + PMMA, PO + PMMA, and R6G + PMMA samples, after prolonged placement in vacuum.

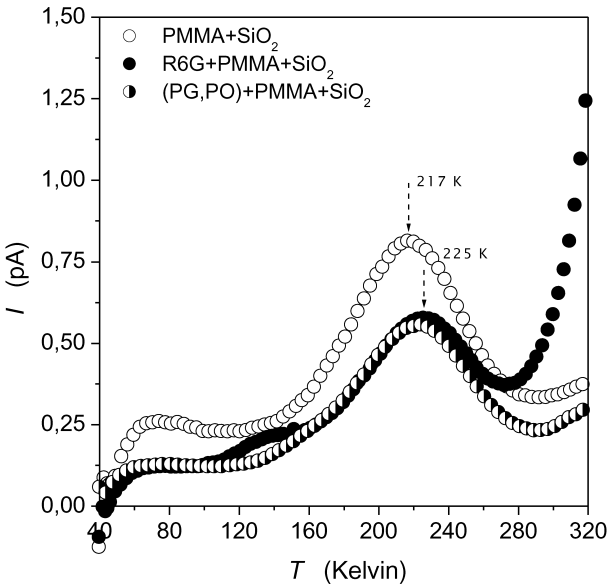


Fig. 3. TSD current spectra of PMMA + $SiO_2$, PG + PMMA + $SiO_2$ and R6G + PMMA + $SiO_2$ samples, after their prolonged placement in vacuum. The TSD current spectra of PO + PMMA + $SiO_2$ (not shown here) and PG + PMMA + $SiO_2$ are similar.

character of the dye salt and is most probably attributed to combined protonic and chloride space-charge-relaxation mechanisms [32].

The potential barrier to the rotational mechanism of the ester carbonyl side groups has a specific intra-molecular part, while the broad distribution in the relaxation parameters is associated with inter-molecular interactions that contribute to the rotational motion. TSD performed in steps enable one to establish whether a dipole distribution arises either from a distribution in activation energies or from one in natural frequencies ($\tau_0^{-1}$), or in both parameters. The so-called step heating or partial heating method [34] is based on the fact that the natural logarithm of the current at the initial slope of the discharge signal is proportional to the apparent activation energy: the steeper the current rises, the higher the activation energy is. In that method the heating is interrupted at increasingly higher temperatures (cut-off temperature, $T_{cut}$). After each interruption the electret is cooled and reheated for another TSD. The distributed polarization is thus investigated in parts: in the first TSD runs the fast groups of dipoles are mobilized while in the subsequent runs at higher temperatures the slower dipoles gain enough mobility to reorient [35]. Fig. 4 shows the variation of the apparent activation energy barriers as a function of $T_{cut}$ in the temperature range of the β relaxation, for the entire range of the investigated materials. The energy values were determined with good accuracy from plots of ln $I$ against $1/T$, where the slope of the straight line obtained equals $-E_a/R$. Especially in the case of the purely organic materials, i.e. pure PMMA and (R6G, PG, PO) + PMMA dye blends, the analysis of the current rises reveals a monotonically increasing dependence [36] of $E_a$ vs. $T_{cut}$ in good agreement with earlier partial heating results for PMMA reported by Vanderschueren [37].

The TSD current signal of the secondary relaxation is slightly broadened in the composite (Fig. 5), especially at its low-temperature side. The observed broadening may be considered confinement effect on the relaxation characteristics of the side-chain mechanism and not an artifact (e.g. due to the contribution of satellite relaxation modes) since the current thermograms used for the comparison have been recorded after prolonged vacuum and thermal treatment of the samples. This procedure ensures the drastic weakening of the low- and high-temperature relaxation modes. In detail, the water-related relaxation mode activates below approximately 0.65 $T/T_{max(\beta)}$, while the low-temperature tail of the primary transition signal (from isotactic sequences of PMMA) is expected above about 1.25 $T/T_{max(\beta)}$.

For a more thorough experimental analysis of the complex TSD β relaxation current signal the thermal sampling (TS) technique has been employed. This technique consists of 'sampling' the relaxation process within a narrow temperature range by polarizing at a temperature $T_p$ and depolarizing at $T_d$ a few degrees lower than $T_p$ and by spanning the entire temperature range of the global TSD current peak with a series of TS measurements. This thermal cycling is not expected to have any influence on the form of the distribution in the case of local β relaxations. On the other hand, the analysis of the TS responses results in an easier interpretation of the TSD current peaks as the current 'samples' are quasi non-distributed. Fig. 6 shows results obtained with PMMA by using the TS technique: approximately single TS responses are isolated in the region of the global TSD β peak. The characteristic relaxation parameters ($E_a$, $\tau_0$) of each thermal sampling band have been determined using fitting procedures described elsewhere [38].

Fig. 7 shows the plots of the image charge $Q$, released from the electrodes during sample heating in each TS scan, as a function of the corresponding $E_a$ parameter for PMMA and PMMA + $SiO_2$. The charge $Q = S/b$, where $S$ is the area of the TS peak and $b$ the heating rate, is representative of the fraction of the dipole population reorienting with a specific energy barrier. The $Q$ vs. $E_a$ plots depict some properties of the distribution function for the apparent energy barriers of the β relaxation mechanism. The distribution function for the secondary relaxation in pure PMMA appears to be symmetric: the number of molecules experiencing a specific energy barrier increases smoothly with $E_a$ up to a maximum value, which corresponds to the characteristic energy barrier $E_a' = 45$ kJ/mol near the maximum of the global β relaxation band, and then shows a gradual drop off. In the composite we observe strong and highly asymmetric broadening of the distribution and an overall increase of the energy barriers. Viewing the secondary local relaxation as a superposition of parallel

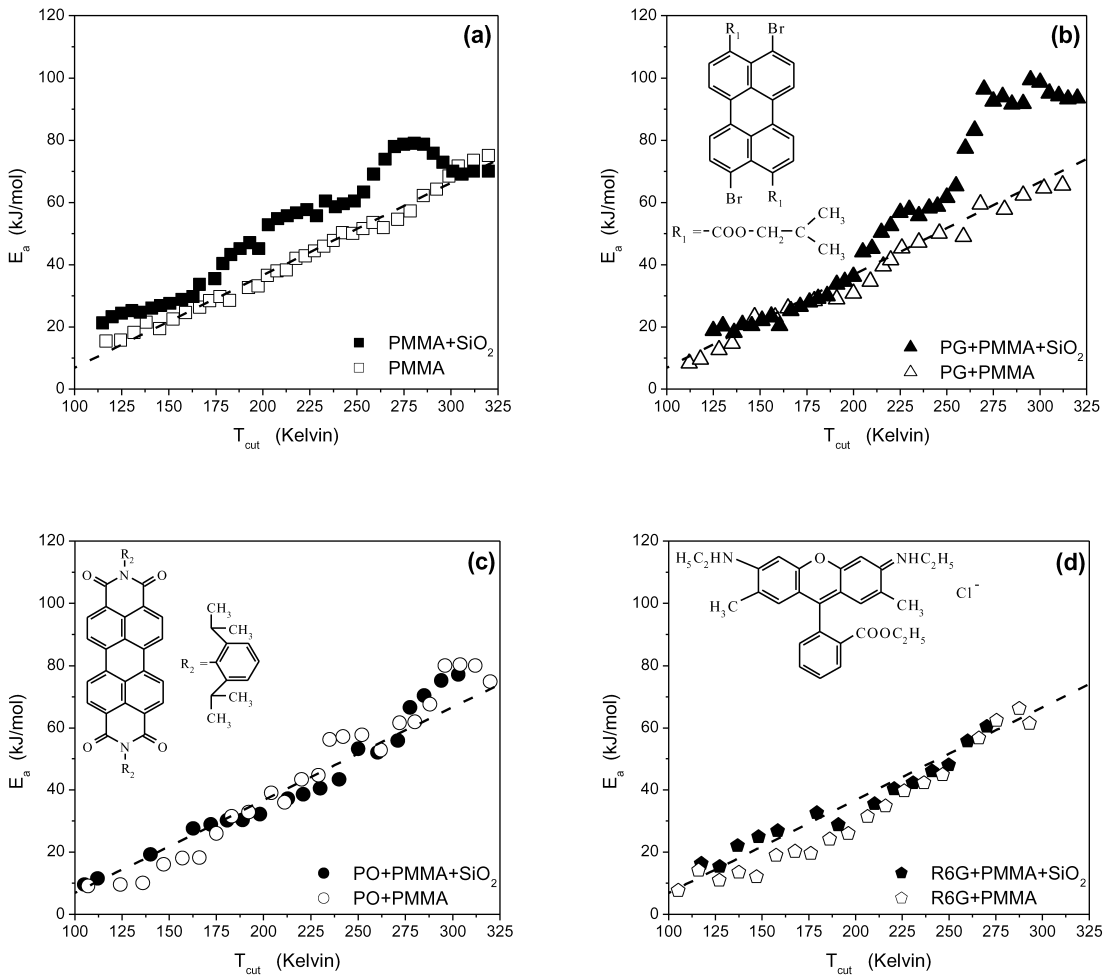


Fig. 4. Plots of the apparent activation energy barriers, $E_a$, as a function of the cut-off temperature $T_{cut}$ recorded for: (a) bulk PMMA and the biphasic PMMA + $SiO_2$ matrix, and their blends with (b) PG, (c) PO and (d) R6G. The chemical structures of each dye are also included in the plot. The least-square fitting curve (- - -) of the $E_a$ vs. $T_{cut}$ dependence for bulk PMMA is given for comparison.

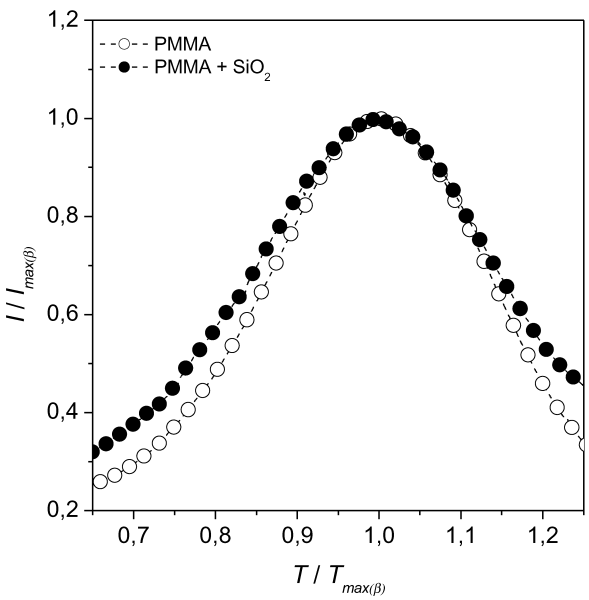


Fig. 5. Reduced current–temperature plots ($I/I_{max(\beta)}$ vs. $T/T_{max(\beta)}$) of the secondary relaxation in PMMA and the biphasic system PMMA + $SiO_2$.

elementary processes, the results shown in Figs. 3 and 5 indicate that in the confined state, the 'faster' modes of the β signal (at $T < T_\beta$) present a relatively more intense contribution to the relaxation strength of the band. Data in Fig. 7 also indicate an increase in the width of the $E_a$—distribution pattern, possibly owing to a broader range of interactions between the carboxymethyl groups of PMMA and the partially hydroxylated silica layer. The difference, $\Delta E_a$, in the energy values at the maximum of the global TSD current peaks is around +10 kJ/mol, in agreement with the partial heating results in Fig. 4. A less significant, and somewhat asymmetric in the case of R6G + PMMA, broadening of the distribution, most likely due to weak guest–host interactions, is also depicted by the $Q$ vs. $E_a$ dependence (Fig. 8) for the purely organic dye blends.

The analysis of the TS peaks, with the estimation of the relaxation parameters ($E_a$, $\tau_0$) for the components of the β relaxation band, revealed another interesting observation. The plots of log $\tau_0$ vs. $E_a$ for several dielectrics demonstrate

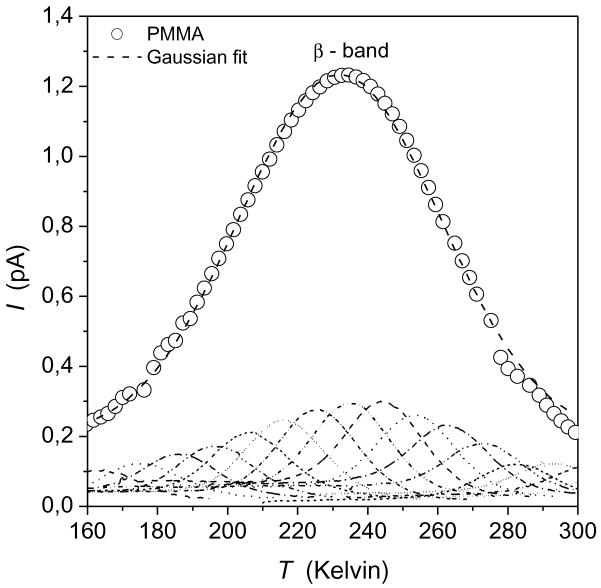


Fig. 6. Global TSD current thermogram obtained with PMMA and some representative TS responses isolated in the region of the β peak (160 K < $T$ < 300 K). The symmetric global β current peak has been fitted to a Gaussian function.

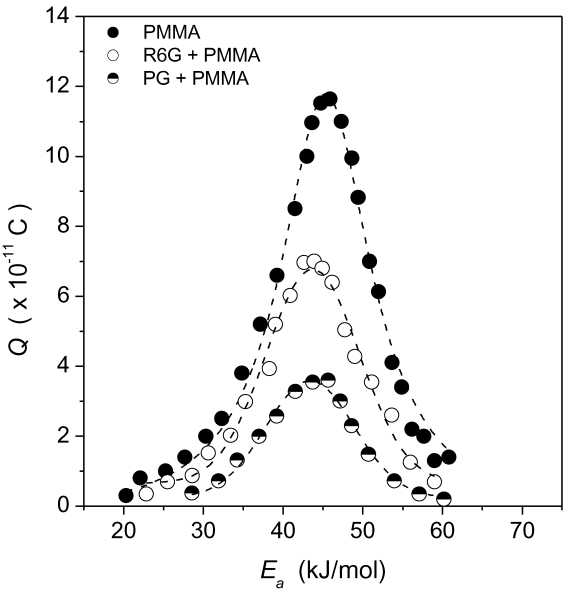


Fig. 8. Plots of the released charge $Q$, in each TS scan, as a function of the apparent activation energy ($E_a$) for bulk PMMA and the blends R6G + PMMA and PG + PMMA.

a linear relationship between log $\tau_0$ and $E_a$, of the type

$$\log \tau_0 = \log \tau_c - \frac{E_a}{\ln(10)RT_c} \quad (4)$$

This relation, known as compensation law, has been observed in many polymeric systems and is under intensive and controversial discussion [39,40]. A representative example of the behavior exhibited by our systems is shown in Fig. 9 for bulk PMMA and the composite PMMA + $SiO_2$. As expected $\tau_0$ decreases as $E_a$ increases.

For PMMA the data can be fitted to the equation

$$\log(\tau_0/s) = -1.759 - 0.127E_a \text{ (kJ/mol)}$$

and in comparison to Eq. (4) we calculate the following phenomenological compensation parameters: $\tau_c = (18 \pm 2) \times 10^{-3}$ s and $T_c = 411 \pm 19$ K. For the biphasic PMMA + $SiO_2$ system the data can be fitted to the equation

$$\log(\tau_0/s) = -3.799 - 0.096E_a \text{ (kJ/mol)}$$

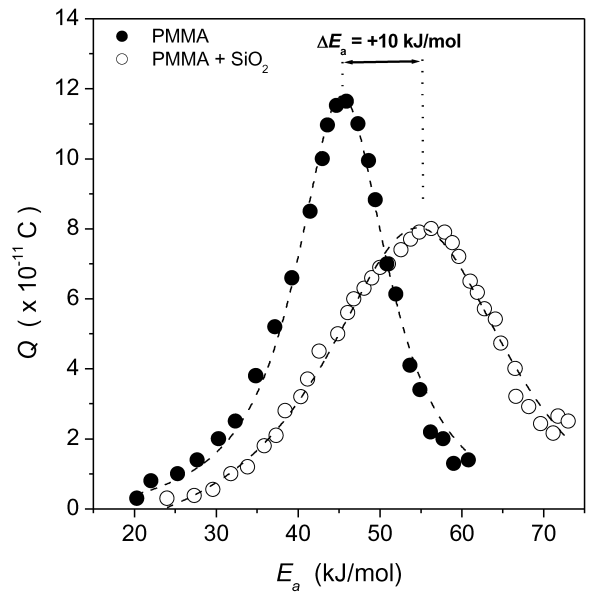


Fig. 7. Plots of the released charge $Q$, in each TS scan, as a function of the apparent activation energy ($E_a$) for bulk PMMA and the biphasic PMMA + $SiO_2$ system.

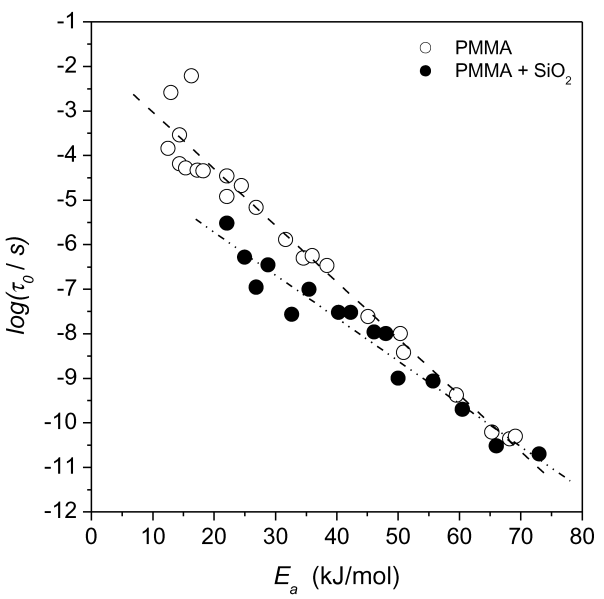


Fig. 9. Plot showing the changes of $E_a$ and log $\tau_0$, determined for each TS response recorded for bulk PMMA and the biphasic system PMMA + $SiO_2$. The dashed lines depict the linear fit of the points to Eq. (4).

which gives $\tau_c = (1.1 \pm 0.3) \times 10^{-4}$ s and $T_c = 544 \pm 26$ K.

Compensation behaviors recorded for primary (α) signals in polymers correlate the compensation temperature $T_c$ with the glass transition or the fictive equilibrium temperatures. However, the observation of a similar effect for local non-cooperative secondary relaxations has no physical meaning. For example, a relation between $E_a$ and $\tau_0$ is anticipated since the values of the activation energy and the inverse frequency factor (at infinite temperature) are interconnected by Eq. (3), which is valid for any TSD current peak. Thus, when the activation energy of the relaxation process increases the pre-exponential factor will decrease necessarily in order to maintain the maximum of the peak in more or less the same temperature region. Irrespective of the existence or not of a true physical meaning for the compensation law, the errors for $T_c$ are too significant to validate the existence of a compensation point for the β relaxation, either in bulk PMMA or the polymer phase confined into porous $SiO_2$.

## 4. Discussion

A direct comparison of the TSD results for the dye-free matrices leads to the following remarks. In the biphasic PMMA + $SiO_2$ system, the increase of the apparent activation energy barriers associated with the side-chains (re)orientation process and the low-temperature shift of the β band, compared to the same mechanism in conventional PMMA, are related to counteracting confinement effects. The first result is attributed to the chemical character of the interacting phases. The electron donor behavior of PMMA, due to the electronegativity of the oxygen and the readily available lone pair electrons in the carbonyl group [41], permits strong acid–base interactions (hydrogen bonds, δH) with acidic solvents (e.g. $CHCl_3$ [42], $CH_2Cl_2$ [43]) or acidic surfaces (e.g. inorganic fillers [44]). The high surface area and surface free energy of the silica gel facilitates a strong interaction of basic PMMA with the silicic acid pore surface [11]. The δH interaction scheme is widely accepted nowadays and has been adopted to explain experimental results of, e.g., Mossbauer [45], Infrared [10,46,47], FT-Raman [10], DRS [13], Differential Scanning Calorimetry (DSC) [15,48] and fluorescence [49] spectroscopy studies. For example, the changes of the vibrational features of silanols on the silica surface and the ester carbonyls from PMMA are indicative of the δH interaction (e.g. a shoulder at 1699 $cm^{-1}$ on the 1725 $cm^{-1}$ band assigned to the stretching mode of the C=O bond is attributed to hydrogen bonded side-groups [14]). In addition, PMMA confined in silica-gels with 5 nm average pore diameters exhibits α transition TSD current signals [38] and DSC exothermic peaks [15], which indicate high-temperature shifts of the glass–rubber transition temperature attributable to an intense PMMA–silica interaction [48].

In view of the above observations, the occurrence of extensive δH interactions (surface or chemical effect) between the ester carbonyls of PMMA and the silicic acid pore surface can give a plausible explanation of the overall increase in the distributed energy barriers (Fig. 4a, [13]). A distinct effect of this interaction should be the deceleration of the (re)orientation mechanism (i.e. decreased relaxation frequencies) and a high-temperature shift of the complex TSD current band. The observation of the opposite phenomenon stresses the significance of the structural confinement effects in the molecular relaxation mechanisms of PMMA polymerized in situ porous silica-gels. The reduction of the polymer's chain entanglements and the increase in the free volume due to the pore-directed polymerization is considered to loosen up several steric hindrances on the rotational motion and bring on increased side-chain molecular mobility (β process). These changes may be used to explain the drastic low-temperature shift of the corresponding TSD current signal. Based on the Eyring's formalism for the relaxation time, the increase in the activation entropy factor ($\Delta S$) is most likely responsible for the downshift of the β signal (Fig. 3, [32]).

Contrarily to the thermal behavior of PMMA in 5 nm silica-gels [15] in biphasic materials with average pore diameters between 10 and 15 nm an approximately 20° decrease of $T_g$ has been recorded [50,51]. Therefore, close relationship appears to exist between the apparent dielectric and thermal behavior of the confined phases and the percentage of lateral groups undergoing strong surface interactions (i.e. the number carboxy–methyl groups at the outer shell of PMMA relative to the total amount). The thicker the inner non-interacting phase of confined PMMA is (e.g. in large-pore confinement environments), the stronger the contribution of structural effects and the speed-up of the overall molecular relaxation times are to be expected.

Phenomenologically contradicting TSD current responses have been recorded between the investigated solid-state dye lasing materials. The dissimilarities are most likely connected to the different microenvironments of the side groups, due to variations in the chemical nature of the organic oligomers and the unlike structural placement of the chromophores in the dye blends. In the purely organic R6G + PMMA blend the strong low-temperature shift of the β band, with no changes in the $E_a$ distribution pattern, indicates the partial coupling [52,53] between the polar chromophores and the side-group rotations due to dipole–dipole interactions. In R6G + PMMA + $SiO_2$ the environment provided for the ester carbonyls of PMMA is drastically different. Viewing the residual water present in the composite system and the hydrophilic nature of the partially densified silica-gel glass [16], water should also be able to compete with basic carbonyls from polymer chains for occupying the surface silanol sites. Due to the insufficient number of acidic sites available for hydrogen-bonding and to a lower degree due to the occupation of some

silanol sites by water molecules, the majority of the carbonyl groups remain unbonded [10]. In the R6G + PMMA + $SiO_2$ system the attachment of the chromophores on the pore surfaces (by a number of weak, i.e. Van der Waal's forces, and stronger interactions, e.g. hydrogen bonds with the silanols) enhances the 'shielding' of the side-groups from the acidic pore surface. The dependence of the magnitude of the low-temperature shift of the band on the extent of the shielding of the side-groups by the dye molecules (proportional to the concentration of the dye [38]) supports the above considerations (Fig. 10). In addition, the decrease of the 'effective' average pore diameters, available for MMA diffusion and PMMA growth, balances the structural (physical) and surface (chemical) effects, as depicted in the similarity of the apparent activation energy distribution patterns in both rhodamine 6G/$Cl^-$ blends and pure PMMA (Fig. 4d).

Blending of the perylene derivatives with PMMA has no effect on the molecular dynamics of the secondary relaxation as these were recorded in the purely organic dye + PMMA blends. In PG + PMMA + $SiO_2$, however, the β relaxation activation energy spectrum exhibits a slight rise above 200 K (Fig. 4b) in agreement to the behavior of the dye-free PMMA + $SiO_2$ matrix (Fig. 4a). A plausible explanation can be based on the fact that the dye molecules and the macromolecular phase are ultimately mixed in the final polymerization product, allowing several hydrogen-bond susceptible sites in both the inorganic ($SiO_2$) and organic (PMMA) glass components. Simultaneously, blending enhances the above effect since even weak molecular interactions between the organic components and steric hindrances exerted by the PG molecules may further reduce the mobility of several lateral groups. Thus, the highly effective surface-chemical interaction and the reduction of the polymer's free volume induce the behavior shown in Fig. 4b. Substitution of perylene orange (Fig. 1c) for perylene green (Fig. 1b) clearly alters the response of the β relaxation mode in the biphasic matrices. This can be tentatively attributed to the differences between the chemical structures of the perylene derivatives: PO has slightly larger length (~10% longer) and four carbonyl groups per molecule, compared to the two carbonyls per molecule of the PG dye. In the former, the carbonyl groups are positioned at phenyl rings in the main body of the molecule (Fig. 1c), while the plane of the bulky alkyl-substituted phenyl rings at the ends is oriented perpendicular to the plane of the four carbonyls. Since the carbonyl group shows the highest tendency for hydrogen bonding interaction with the surface silanol groups of $SiO_2$ there appears to be high possibility for PO orientation parallel and close to the pore walls. Thus, compared to perylene green the orange derivative shields more effectively the lateral groups of PMMA from interacting with the acidic $SiO_2$ surface, in agreement to the behavior depicted by the $E_a$ vs. $T_{cut}$ trends in Fig. 4c. A comparison of the high-temperature TSD responses in the region of the α relaxation mode would be very beneficial for a more thorough investigation of the interactions in each dye blend. However, since the organic dyes become highly unstable in the temperature region of the TSD current α peak (between approximately 373 and 400 K, for low-temperature free radical polymerization products) such experiments have not been attempted.

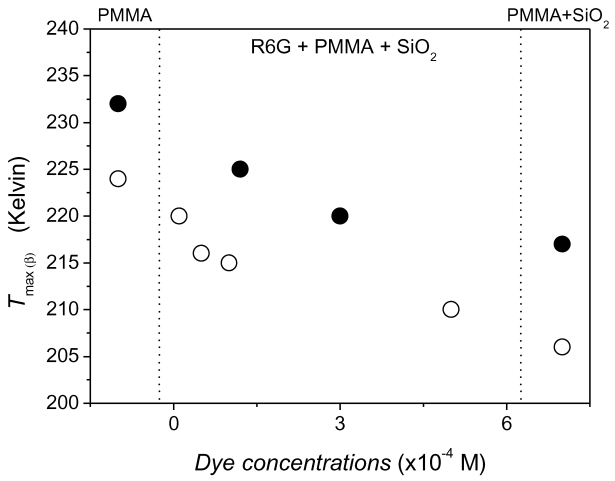


Fig. 10. Variation of the position of the TSD current peak of the secondary relaxation of PMMA in bulk PMMA and the composites R6G + PMMA + $SiO_2$ and PMMA + $SiO_2$, prepared with different initiators: (●) benzoyl peroxide and (○) azo-bis-isobutyro-nitrile.

The special physicochemical properties of the PMMA and PMMA + $SiO_2$ matrices that differentiate their thermo-stimulated discharge current responses are also expected to have direct impact in their lasing characteristics. In general, the changes in the lasing properties of a dye immersed in different carriers, such as the organic solvents and solid-state hosts, can be rationalized in terms of both the accompanying changes in the environmental polarity and variations in the immediate environment of the chromophores. As regards the highly polar and ionic dye rhodamine 6G/$Cl^-$, in passing from the typical liquid solution media to materials with increased matrix rigidity a substantial hindering of the internal rotational relaxation modes of the dye is anticipated [3,54]. The stabilization of the fluorescing component is an immediate consequence [7,55]. In dielectric spectroscopy studies the reduction of the effective 'free-volume' which is available for the (re)orientation of the dye molecules or the direct covalent bonding of the dye to polymeric chains [56] can be readily monitored through their effect on the molecular mobilities of the relaxing entities of the polymer matrix. In the present study, the absence of any distinct TSD current band due to the intramolecular mobility of the polar R6G chromophores suggests that the effective 'immobilization' of the R6G molecules at the organic-silica-gel interface hinders the dielectrically active rotations of the polar carboxyethyl group, in the phenyl side-group of rhodamine 6G. A rigid $SiO_2$ cage is expected to quench, to a greater degree, the reorientation mechanism of the chromophore. This has been experimentally verified by several optical studies [3,57]

which demonstrate that the 'sol–gel philic' R6G dye shows better photostability and better radiation efficiency in the sol–gel process derived silica glass, compared to PMMA + $SiO_2$ and bulk PMMA. It should be noted at this point that thermoplastic materials like PMMA present a relatively loose arrangement of the macromolecular chain structure. The mobility of the chains in relatively loosely packed (low density) regions within PMMA is considered responsible for intense structural relaxation phenomena, recorded even at temperatures far below its glass–rubber transition temperature. Intense lasing function is accompanied by a rise in the temperature of the optical material that activates a number of local-chain and long-range relaxation modes of the polymer backbone with parallel consequences on both the dimensional stability and the lasing efficiency of the system. Increased laser damage thresholds have been recorded for PMMA modified by the addition of ethyl alcohol [5,58], probably for reasons related to the strong interactions of the dye with the polar alcoholic phase.

Contrarily to the xanthine chromophore the 'sol–gel phobic' perylene derivatives perform better in the organic glass (PMMA) and the biphasic PMMA + $SiO_2$ hosts [6], compared to pure $SiO_2$ or the organically modified silicates (ormosils [59]) hosts. Given the fact that in the first two matrices the immediate environment of the chromophores primarily consists of PMMA chains the relative gains of using PMMA + $SiO_2$ over PMMA have to be related with special features of the inorganic component, such as its higher thermal conductivity (that reduces thermal lensing effects) and the improved transparency in the UV and IR regions over pure PMMA. The silicon oxide skeleton and the hydrogen bonds in the silica–PMMA interface are also expected to influence several fluorescence characteristics [49].

## Acknowledgements

Thanks are due to Dr Mark D. Rahn (Laser Photonics Group, Physics and Astronomy Department, University of Manchester) for supplying the dye + polymer and composite blends and for participating in valuable discussions.

## References

[1] Schäfer FP, editor. Dye lasers. Topics in applied physics, vol. 1. Berlin: Springer; 1990.
[2] Hench LL, West JK. Chem Rev 1990;90:33–72.
[3] Rahn MD, King TA. Appl Opt 1995;34:8260–71.
[4] Avnir D, Levy D, Reisfeld R. J Phys Chem 1984;88:5956–9.
[5] Wadsworth WJ, Griffin SM, McKinnie IT, Sharpe JC, Woolhouse AD, Haskell TG, Smith G. J Appl Opt 1999;38:2504–9.
[6] Rahn MD, King TA. SPIE Sol–Gel Opt III 1994;2288:382.
[7] Deshpande AV, Namdas EB. J Lumin 2000;91:25–31.
[8] Yariv E, Schultheiss S, Saraidarov T, Reisfeld R. Opt Mater 2001;16:29–38.
[9] Nogues JLR, Moreshead WV. J Non-Cryst Solids 1990;121:136–42.
[10] Li XC, King TA. J Sol–Gel Sci Technol 1995;4:75–82.
[11] Nobrega MC, Gomes LCF, LaTorre GP, West JK. Mater Charact 1998;40:1–5.
[12] Abramoff B, Klein LC. SPIE Sol–Gel Optics 1990;1328:241–8.
[13] Kalogeras IM, Vassilikou-Dova A, Neagu ER. Mater Res Innovations 2001;4:322–33.
[14] Li XC, King TA, Pallikari-Viras F. J Non-Cryst Solids 1994;170:243–9.
[15] Pallikari-Viras F, Li XC, King TA. J Sol–Gel Sci Technol 1996;7:203–9.
[16] Wallace S, Hench LL. J Sol–Gel Sci Technol 1994;1:153–68.
[17] El-Shahawy MA, Mansour AF, Hashem HA. Indian J Pure Appl Phys 1998;36:78–84.
[18] El-Shahawy MA. Polym Test 1999;18:389–96.
[19] El-Shahawy MA. Polym Test 2000;19:821–9.
[20] Lei D, Runt J, Safari A, Newnam RE. Macromolecules 1987;20:1797–801.
[21] Moller K, Bein T, Fischer RX. Chem Mater 1998;10:1841–52.
[22] Kranbuehl D, Knowles R, Hossain A, Gilchriest A. J Non-Cryst Solids 2002;307:495–502.
[23] Nieh MP, Kumar SK, Ho PL, Briber RM. Macromolecules 2002;35:6384–91.
[24] Schönhals A, Goering H, Schick C. J Non-Cryst Solids 2002;305:140–9.
[25] McCoy JD, Curro JG. J Chem Phys 2002;116:9154–7.
[26] Anastasiadis SH, Karatasos K, Vlachos G, Manias E, Giannelis EP. Phys Rev Lett 2000;84:915–8.
[27] Esnouf S, Benneu F, Enzel P, Bein T. Phys Rev B 1997;56:12899–904.
[28] Pelster R. Phys Rev B 1999;59:9214–28.
[29] Neagu RM, Neagu ER, Kalogeras IM, Vassilikou-Dova A. Mater Res Innovations 2001;4:115–25.
[30] Van Turnhout J. Thermally stimulated discharge of polymer electrets. Amsterdam: Elsevier; 1975.
[31] Vanderschueren J, Gasiot J. Field-induced thermally stimulated currents. In: Sessler GM, editor. Topics in Applied Physics. Berlin: Springer; 1980.
[32] Kalogeras IM, Vassilikou-Dova A. J Phys Chem B 2001;105:7651–62.
[33] Schmidt-Rohr K, Kulik AS, Beckham HW, Ohlemacher A, Pawelzik U, Boeffel C, Spiess HW. Macromolecules 1994;27:4733–45.
[34] Creswell RA, Perlman MM. J Appl Phys 1970;41:2365–75.
[35] Starkweather HW. Macromolecules 1988;21:1798–802. Starkweather HW. Macromolecules 1990;23:328–32.
[36] Dargent E, Kattan M, Cabot C, Lebandy P, Ledru J, Grenet J. J Appl Polym Sci 1999;74:2716–23.
[37] Vanderschueren J. J Polym Sci Phys 1977;15:873–80.
[38] Kalogeras IM, Neagu ER, Vassilikou-Dova A, Neagu RM. Mater Res Innovations 2002;6:198–205.
[39] Moura Ramos JJ, Mano JF, Sauer BB. Polymer 1997;38:1081–9.
[40] Rault J. J Non-Cryst Solids 1998;235–237:737–41.
[41] Allara DL, Fowkes FM, Noolandi J, Rubloff GW, Tirrell MV. Mater Sci Engng 1986;83:213–26.
[42] Bistac S, Schultz J. Prog Org Coat 1997;31:347–50.
[43] Hanumantha K, Forssberg KSE, Forsling W. Colloid Surf A 1998;133:107–17.
[44] Iler RK. The chemistry of silica: solubility, polymerization, colloid and surface properties and biochemistry. New York: Wiley; 1979.
[45] Leidheiser Jr. H, Deck PD. Science 1988;241:1176–81.
[46] Allara DL, Wang Z, Pantano CG. J Non-Cryst Solids 1990;120:93–101.
[47] Balastre M, Berquier JM. Langmuir 1999;15:8691–4.
[48] Porter CE, Plum FD. Macromolecules 2000;33:7016–20.
[49] Gvishi R, Narang U, Bright FV, Prasad PN. Chem Mater 1995;7:1703–8.
[50] Pope EJA, Asami M, Mackenzie JD. J Mater Res 1989;4:1018–26.

[51] Abramoff B, Klein CL. In: Uhlmann DR, Ulrich DR, editors. Ultrastructure processing of advanced materials. New York: Wiley; 1992. p. 401.
[52] Brower SC, Hayden LM. J Polym Sci Phys 1998;36:1013–24.
[53] Strutz SJ, Brower SC, Hayden LM. J Polym Sci Phys 1998;36: 901–11.
[54] Hu LL, Jiang ZH. Opt Commun 1998;148:275–80.
[55] Costela A, Garcia-Moreno I, Figuera JM, Amat-Guerri F, Sastre R. Laser Chem 1998;18:63–84.
[56] Arbeloa FL, Arbeloa TL, Arbeloa IL, Costela A, Garcia-Moreno I, Figuera JM, Amat-Guerri F, Sastre R. Appl Phys B 1997;64:651–7.
[57] Reisfeld R, Zusman R, Cohen Y, Eyal M. Chem Phys Lett 1988;147: 142–7.
[58] Somasundaram G, Ramalingam A. J Photochem Photobiol A 1999; 125:93–8.
[59] Ormosils are non-porous hybrid organic/inorganic glass materials in which the inorganic and organic components are covalently bonded to each other. Compared to the usual silica-gel, ormosil is a less polar medium, which in most cases favors the monomeric form of the doped dye and prevents dimerization i.e. see Schmidt H. J Non-Cryst Solids 1985;73:681–91. Schmidt H. J Non-Cryst Solids 1989;112:419–23.